Submission code: ARQG68MZR9

See this and other abstracts on our website: https://home.sbgf.org.br/Pages/resumos.php

Target-oriented time-remigration: application to surface and synthetic VSP data

Carlos Augusto Ferreira (ANM), KARINA GOMES (Oriti Solutions), Karina Gomes (Oriti Solutions), Alexandre Oliveira

Target-oriented time-remigration: application to surface and synthetic VSP data

Carlos A. S. Ferreira, Agência Nacional de Mineração – ANM/MT/Brazil
Karina P. Gomes, Oriti Solutions/SP/Brazil
Alexandre S. Oliveira, Rio de Janeiro/Brazil – independent researcher

This paper was prepared for presentation during the 18th International Congress of the Brazilian Geophysical Society held in Rio de Janeiro, Brazil, 16-19 October 2023.

Abstract

In this work we report on the application of a Kirchhoff-type time-remigration procedure, this time applied to 2-D, time-domain, synthetic vertical seismic profiling (VSP) data for target-oriented imaging. Unlike previous results of Kirchhoff remigration performed in the time domain in full-fold common-offset sections (i.e., surface data), we have attained so far only *mapping* migration results for VSP. Due to the geometry of VSP acquisition, remigration is by then performed only in a non-rotated system.

Introduction

In several situations while prospecting for oil and gas it is necessary to establish targets for posteriori appraisals or structural interpretation in the vicinity of an exploration well. This situation may be used even for the cases of monitoring or for reducing risks. These are examples of cases in which target-oriented imaging is an important tool for exploration or production and development (E&P) phases. Target-oriented processing can enhance resolution and reduce artifacts within the target area, particularly when dealing with complex overburden or when data outside the target is noisy (OpenAI, 2025). Considering that the location of the well had already been chosen based on surface seismic images, Stewart (2001) states that in situ rock properties in depth (e.g., velocity, impedance, anisotropy and attenuation), wave propagation (signatures, multiples, conversions), and reflectivity in depth, all these features must be assessed for any further surface seismic data processing and interpretation. VSP is one technique used for target-oriented imaging.

Vertical seismic profiling (VSP) presupposes the deployment of several sensors down along a vertical or deviated borehole profile and near one target area. A near surface source is then fired and several reflected, diffracted, or direct events are recorded per receiver, along traveltime curves. The source may remain fixed near the borehole or displaced several meters away. To each one of these sources positioning, one common-shot vertical profile is generated. The process of gathering data proceeds until a certain range of illumination per shot is obtained for posteriori processing procedures.

The next step after acquisition is the proper imaging of the VSP data. Normally VSP seismic data is processed and migrated independently from surface data, the VSP image then spliced into surface seismic result for interpretation and correlation (Grech et al., 2001). Harwijanto et al. (1987) states that a relatively and unexplored aspect of VSP data is the potential to obtain structural information from the subsurface around the borehole. Since the number of receivers deployed in a borehole is limited (e.g., one trace is recorded per depth per shot), the aperture of VSP data is not enough to prevent migration artifacts during imaging process. Another feature is that the so-called image locus of VSP migration is represented by many rotated ellipses intercepting one diffraction position (Harwijanto et al., 1987), forming a noise caused by migration trails of the boundary shots on the final imaging (Li et al., 2023).

In this work we demonstrate the use of target-oriented imaging using remigration theory (Hubral et al., 1996; Tygel et al., 1996). The procedure is performed in the time domain (Oliveira et al., 2023). We decided to investigate this feature since time remigration – in our approach, an one-step migration/demigration procedure, given by a double integral – is computational demanding when a full processing is applied to an input, e.g., common-offset section. Reducing the computational effort in this case means reducing the size of the areas of targets being imaged. For this purpose, we have chosen two examples that exemplifies the use of target-oriented imaging: application to surface data and VSP. All examples are compared to conventional Kirchhoff migration in the time domain.

Method

Kirchhoff-type remigration theory

Kirchhoff depth-remigration was kinematically discussed in Hubral at al. (1996b) and mathematically shown in Tygel et al. (1996). In these works, true-amplitude remigration is achieved by chaining 3-D weighted diffraction-stack migration and isochrone-stack demigration mathematical operators. In terms of reflection imaging, it represents one method developed to solve specific imaging problems, among them the one that deals with “the updating of a *depth-migrated* seismic image according to a different or improved macro velocity model” (Hubral et al., 1996 a,b).

In Oliveira et al. (2023) remigration was recast in the time domain as an *imaging* procedure. Physically, it is a chained one-step stacking procedure that updates one time-migrated result of a seismic section using two different velocity models, considering as input one vintage time-migrated section. Mathematically, it is represented by a weighted double integral acting upon an input time-migrated data. Geometrically, it is a relative one-step migration/demigration procedure that refocuses time-

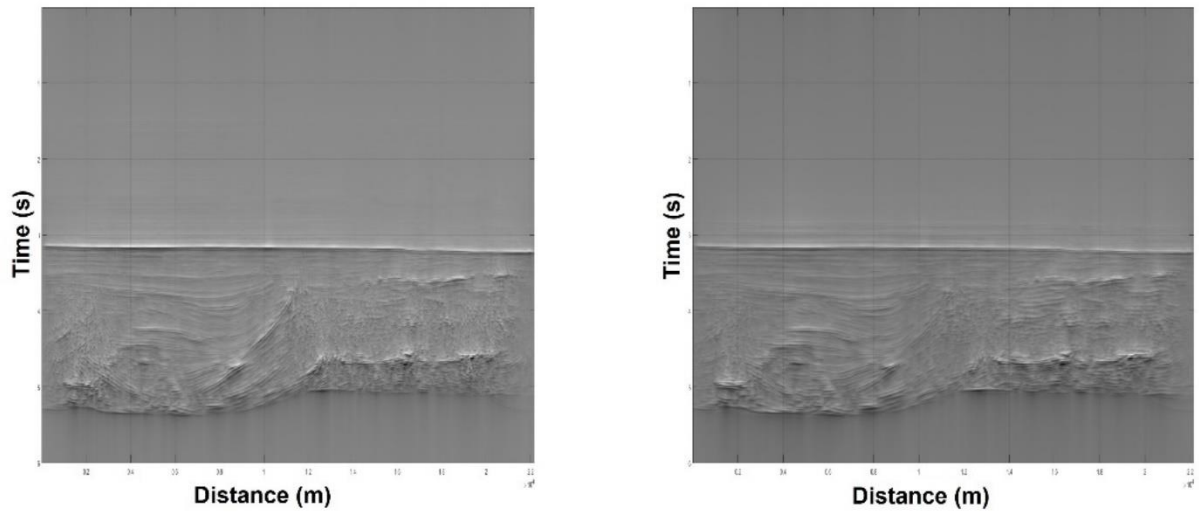

Figure 1 – Shaded relief images of a marine section depicting a presalt target, after Kirchhoff-type imaging procedures.

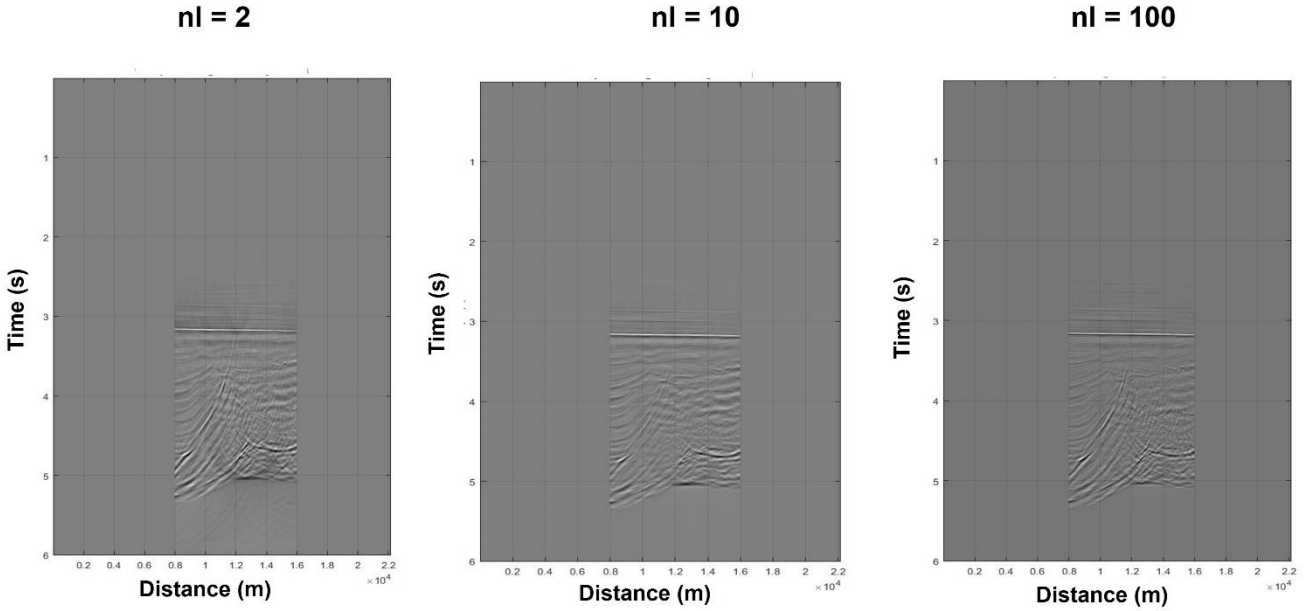

Figure 2 – Target-oriented Imaging using a remigrated image from **Figure 1**. The target here is the left flank of the salt wall, together with layers located bellow the salt body. The dimensionless parameter *nl* above each subfigure indicates one index that control the inner aperture of the demigration operator during the remigration operation.

migrated reflections in the following manner: first, a Huygens curve in 2-D maps common-tangent reflection points inside an aperture *A* through diffraction, using an updated velocity; and second, a relative (and spatially limited) demigration ellipse simulates at each mapped reflection location a mispositioned amplitude in space-time, using a vintage velocity. Currently, we advocate the use of this velocity-continuation procedure in the time domain along a common-offset section. The task of imaging after full processing in the time domain may completed with a posteriori depth transformation, caring for the proper velocity in the transformation.

In the examples that follows a tilde symbol ("~") over functions and variables refer to the output model, including spatial positions, time coordinates and velocities. The remaining variables and functions without tildes refer to the input model, also including spatial positions, time coordinates and velocities. The input and output model both consider an arbitrary, single fold measurement configuration (i.e., sources and receivers are single pairs; see Tygel et al., 1996) of point sources and receivers distributed along the Earth surface, the location of them are described by a 2-D vector parameter, $\vec{\xi} = (\xi_1, \xi_2)^T$. When

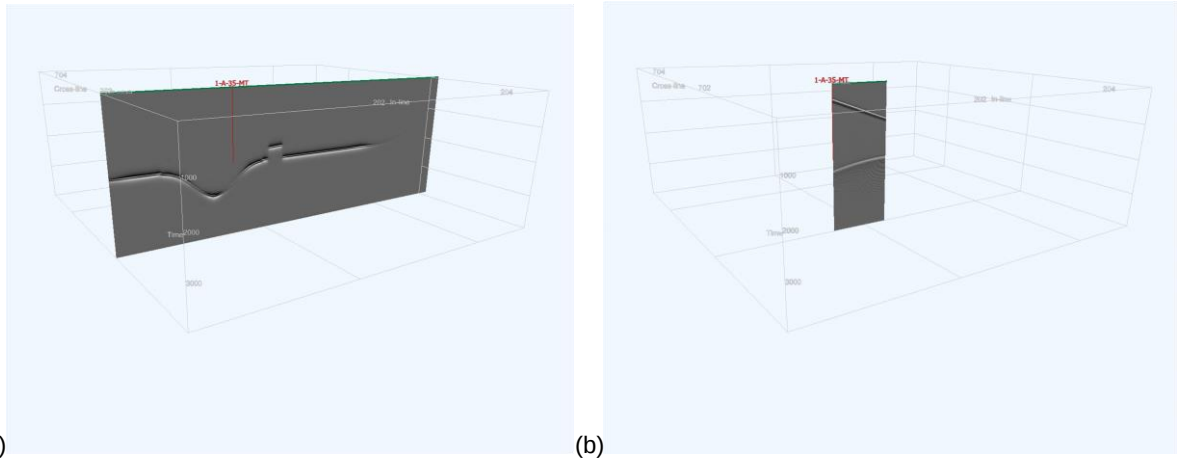

Figure 3 – Synthetic VSP example depicting one exploration well drilled in a sedimentary basin. (a) The main structure is represented by a syncline that is normal faulted somewhere along its horizon. Well 1-A-35-MT was drilled near the flank of the structure and of the fault. (b) Zero-offset VSP data simulated to help interpretation along the structure, including the area near the fault.

referred freely, vector parameter $\vec{\boldsymbol{\xi}}$ varies in *A*, called migration aperture; or when referred specifically, as a stationary point, it determines an aperture constrained by a specific condition.

One more assumption is necessary for all the examples in this work. In the case of all remigrated results, one must assume that the final imaged section obtained was velocity continued following the procedures described in Oliveira et al. (2023), since these results are compared to the direct Kirchhof migration.

Stacking integral

Similar to Kirchhoff-type theory described in Tygel et al. (1998) and Schleicher and Bagaini (2003), for each point $(\tilde{x}, \tilde{\tau})$ in the output time-remigrated section to be simulated, the stack result $\tilde{I}(\tilde{x},\tilde{\tau})$ is obtained by a weighted stack of the input data, represented by the following integral:

$$\tilde{I}(\tilde{x},\tilde{\tau}) = \frac{1}{\sqrt{2\pi}}\int_A \, dx\, K_{RM}^{(2.5D)}(x;\tilde{x},\tilde{\tau})\partial_t^{\frac{1}{2}} I(x,t)|_{t=t_{RM}}(x;\tilde{x},\tilde{\tau}), \quad (1)$$

where $I(x,t)$ is the input time-migrated seismic section that is to be weighted by $K_{RM}^{(2.5D)}(x;\tilde{x},\tilde{\tau})$ and then summed up along the stacking line or inplanat $t = t_{RM}(x;\tilde{x},\tilde{\tau})$ (Tygel et. al, 1996). Both functions are dependent on the point $(\tilde{x}, \tilde{\tau})$ where the stack is to be placed, and on the variable x that specifies the location of the traces being summed in the stack. Moreover, *A* denotes the (spatially limited) aperture of the stack, the range of midpoints (in a common-offset gather) available in the time-migrated input section, $I(x,t)$. Finally, the time-reverse half-derivative

$$\partial_{-t}^{1/2}[f(t)] = \frac{1}{\sqrt{2\pi}}\int_{-\infty}^{+\infty}|\omega|^{\frac{1}{2}} e^{-i\frac{\pi}{4}sign(\omega)} F(\omega)e^{-i\omega t}d\omega \quad (2)$$

is applied to correct the pulse shape. The stacking line $t = t_{RM}(x;\tilde{x},\tilde{\tau})$ is defined by the kinematics of the operation, and the weight-function $K_{RM}^{(2.5D)}(x;\tilde{x},\tilde{\tau})$ will be determined by the desired amplitude behavior.

Eq. (1) is called single solution since it directly relates one input vintage time-migrated seismic section, $I(x,t)$, to its counterpart $\tilde{I}(\tilde{x},\tilde{\tau})$ in the new output domain. This is just possible because it is assumed the a known inplanat $t_{RM}(x;\tilde{x},\tilde{\tau})$ is considered also known in the input domain, relating both sections, respectively, through a stacking curve. In our examples, however, we use the following double integral:

$$\tilde{I}(\tilde{x},\tilde{\tau}) = \frac{1}{\sqrt{2\pi}}\iint_A \, d\xi dx\, K_{RM}^{(2.5D)}(x;\tilde{x},\tilde{\tau})\dot{I}(x,t)|_{t=t_{RM}}(x;\tilde{x},\tilde{\tau}) \, , \quad (3)$$

which is more suitable for numerical computations. The dot over the input section $I(x,t)$ represents a time derivative. Eq. (3) is called one-step chained solution (Oliveira et al., 2023).

Depth remigration as originally described in Hubral et al. (1996b) or in Tygel et al. (1996) may be seen effectively as a "migration of a diffraction", in the following sense: a diffraction surface is generated from the output domain using a more accurate velocity field and this curve is migrated to the input domain with a less accurate velocity field. The resulting surface/curve is the inplanat (or stacking surface/curve) for the remigration process. In other words, considering two velocity fields (one less accurate in the input domain and other more accurate in the output domain), it is possible to *re*migrate (or velocity-continue) one event towards its true position in depth or in time.

In the time domain, the same procedure is mathematically described in one step by Eq. (3).

Kirchhoff remigration approximation for the VSP case

To understand how an imaging operator works regarding its *action* in the output domain, one must study its impulse response. This section then discusses the impulse response for the case of VSP seismic, which we shall show is represented by a set of rotated ellipses. The discussion will be held first from the Kirchhoff migration point of view.

For the case of Kirchhoff migration, when dealing with surface seismic, the image locus for a sample of reflection data are ellipses with source and receiver as foci. In the special case of VSP imaging, the image locus are still ellipses, but this time they are rotated, following the line that connects the source located near the surface of the acquisition and the receiver in depth along the profile of the borehole. In this case, Kirchhoff migration case can correctly handle the VSP geometry.

Now consider the case of a point diffractor in the output domain, in which a more accurate velocity field is available for updating. Considering the VSP geometry, the diffraction traveltime for this point is given by:

$$\tilde{\tau}(z_G;\tilde{x},\tilde{\tau}) = \frac{1}{\tilde{v}_{RMS}}\sqrt{\left(\frac{\tilde{v}_{RMS}\tilde{\tau}}{2}-z_S\right)^2+(\tilde{x}-x_S)^2}+ \frac{1}{\tilde{v}_{RMS}}\sqrt{\left(\frac{\tilde{v}_{RMS}\tilde{\tau}}{2}-z_G\right)^2+(\tilde{x}-x_G)^2}. \quad (4)$$

A 2.5-D Kirchhoff migration of a sample located along this diffraction traveltime surface, where $U(z,t)=A_0\delta(z-z_G)\delta(t-\tilde{\tau}(z_G;\tilde{x},\tilde{\tau}))$ is an ideal impulse, yields the following response in the output domain that is proportional to:

$$I(x,\tau)\sim\delta^{\frac{1}{2}}(\tau_D(z_G^*;x,\tau)-\tilde{\tau}(z_G^*;\tilde{x},\tilde{\tau})), \quad (5)$$

which is a fractional derivative of a Dirac delta function. The locus of this impulse response is given by a rotated ellipse:

$$\frac{(\frac{v_{RMS}\tau}{2}-\xi_2)^2}{\gamma_0/\gamma_2}+\frac{(x-\xi_1)^2}{\gamma_0/\gamma_1}+\frac{2h_1h_2}{\gamma_0}(\frac{v_{RMS}\tau}{2}-\xi_2)(x-\xi_1)=1. \quad (6)$$

The following definitions for the quantities appearing in Eq. (6) holds:

$$\gamma_0=(\frac{v_{RMS}\tilde{\tau}_D}{2})^2\left[(\frac{v_{RMS}\tilde{\tau}_D}{2})^2-h_1^2-h_2^2\right],$$
$$\gamma_1=(\frac{v_{RMS}\tilde{\tau}_D}{2})^2-h_1^2, \quad (7)$$
$$\gamma_2=(\frac{v_{RMS}\tilde{\tau}_D}{2})^2-h_2^2.$$

Here, ξ_1 and ξ_2 are midpoint coordinates, and h_1 and h_2 are half-offset coordinates, for all sources and receivers following the VSP acquisition geometry. In this context, it must be considered that ξ_1 is fixed (well and source *x*-locations are constants), while ξ_2 varies with the depth of each receiver. The same is true for half-offset coordinates. One must notice the difference between coordinates and parameters belonging to the input and output domains (with or without tildes), respectively. It must be noticed that Eq. (6) is a special case of the impulse response for surface seismic, in which ξ_2 and h_2 are both zero.

To correctly use Eq. (3) for the VSP geometry one *should* account for the diffractions along the receivers inside the borehole, for each varying ξ_2 and fixed ξ_1, respectively. Or one should rotate the coordinate system and relate rotated coordinates with unrotated ones. However, the profile of the VSP data is not in the same direction of the output domain, presently prevailing the use of this procedure as an *imaging* tool, just as a *mapping* tool (Hubral et al., 1996b). In the present work, this fact was overcome replacing for now diffraction (4) by the output sample $\tilde{\tau}$ in the inplanat $t_{RM}(x;\tilde{x},\tilde{\tau})$ (Oliveira et al., 2023).

Target-oriented imaging results

Surface data example – Campos Basin, Brazil

Figure 1 shows two 2-D shaded relief images of a seismic section after Kirchhoff-type imaging procedures. In (a) we have a common and well-known Kirchhoff time migration, whereas (b) is a Kirchhoff time remigration of the same

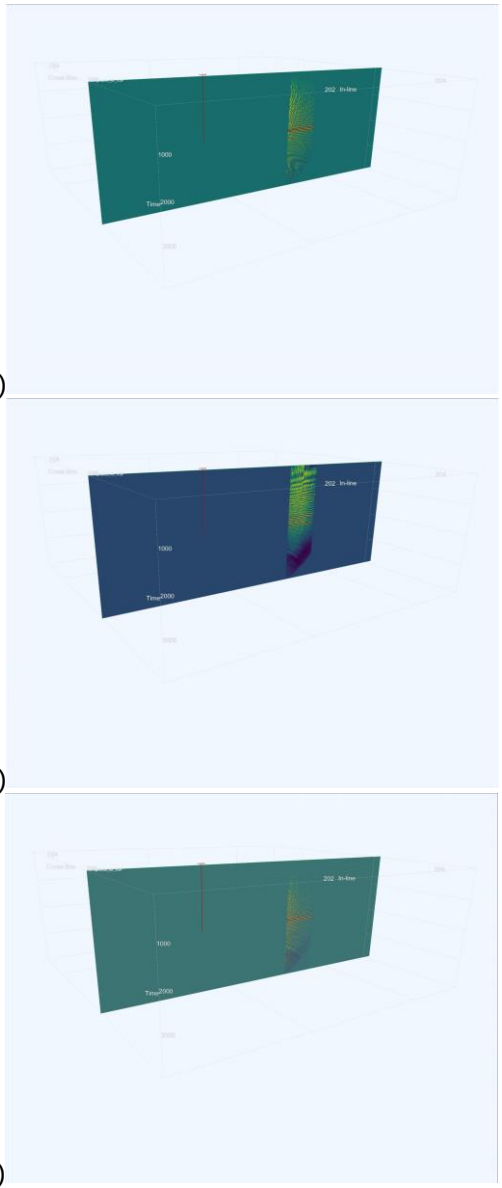

Figure 4 – Imaging results of the VSP data of Figure 3. (a) Conventional Kirchhoff time migration. (b) Kirchhoff remigration using the single solution Eq. (1). (c) Kirchhoff remigration using the one-step solution, Eq. (3).

common-offset input section, following the approach described in Oliveira et al. (2023). The imaged area here was obtained from a marine 2-D survey representative of the so-called “Brazilian presalt”, located in Campos Basin, Brazil.

We have selected this example to show one target-oriented imaging using surface data. **Figure 2** then depicts three subfigures of one selected target of the input section of **Figure 1**, composed of the left flank of the salt body and some layers located just below the salt wall. In theses subfigures one may notice differences in each target image regarding the presence of artifacts (“smiles”) and lateral resolution of some reflections representing events,

including those ones that may be picked inside the salt body and below, along the so called presalt section.

The index parameter *nl* in each subfigure represents one dimensionless number that constrains the inner aperture limit for the demigration operator inherent in the composite aperture *A* in Eq. (3). As this index increases, the aperture of the remigration operator becomes smaller, as well as the computational effort of the process. Also, this feature is directly related to the number of artifacts present in the results, as well as it is proportional to the lateral resolution obtained in the final results. In our examples, *nl* = 10 was chosen as the most effective for processing this specific data regarding computational burden and quality obtained. Also, the resolution of each image is also related to the choice of the index parameter. In this example we can say that the remigration algorithm with the appropriate aperture was effective in imaging all the features of the salt body and the layers just below it along the target zone selected for interpretation.

VSP synthetic data

We have simulated that a well coded 1-A-35-MT was drilled in a sedimentary basin in Mato Grosso, Brazil, prospecting for oil and gas. The main structure investigated was that of a syncline, towards which some possible layers are pinching near its right flank in the inner minibasin. Also, surface seismic revealed that a normal fault is another potential trap for other features nearby, resulting in two (also potential) reservoirs. **Figure 3a** depicts a 3-D perspective of a shaded-relief time-migrated section together with the vertical profile of the well plotted in red. This section may represent any 2-D section or any possible inline or crossline belonging to a 3-D land survey.

For this example, a zero-offset VSP survey was realized to help understand several features near the well (**Figure 3b**). The well is located at 3.0 km from the onset of the section and the VSP source is located 3.01 km to the East of the well. Receivers inside the well are positioned at every 25 m, beginning at depth level 1.0 km, with final depth level at 2.5 km, totaling 60 receivers. In the numerical modeling, only direct and diffracted waves traveltimes were effectively computed.

For convenience, in this picture the VSP common-shot gather is seen with its time axis in the same direction as the time-migrated section. Since for this case the only interface is the top of the syncline structure and the top of the normal fault, the main objective of the VSP imaging is to map sections of the syncline illuminated by the survey using any migration algorithm. Conventional (diffraction-stack) Kirchhoff time migration was then realized and after a shaded-relief processing was executed to enhance lateral resolution. The result is high-quality final image for interpretation.

Figure 4 depicts the imaging results for (a) conventional (diffraction stack) Kirchhoff time migration, (b) Kirchoff time remigration using Eq. (1) (single solution), and (c) Kirchhoff one-step remigration using Eq. (3). Except for the conventional Kirchhoff algorithm, which can handle the VSP geometry and is able to afford for its wavefield propagation (i.e., source at the surface and receivers inside the well profile), in this work remigration was

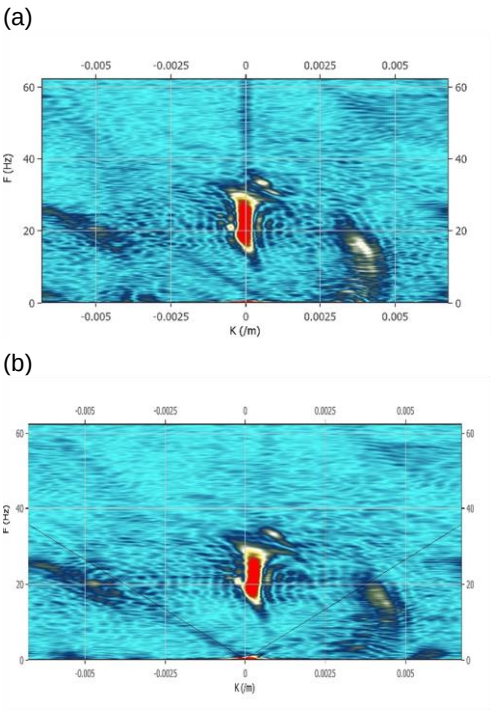

Figure 5 – FK spectra of two results in Figure 4: (a) after conventional Kirchhoff migration; and (b) after Kirchhoff remigration using Eq. (3).

performed for *mapping* purposes. For *imaging* purposes, remigration must be performed in rotated coordinates. This feature is particularly true in the single examples presented here since it virtually accommodated the dips associated with the interval imaged, which are zero. It is visually clear that result (a) is the ideal one presenting the best lateral resolution, although it suffers from poor interference above the section imaged. Image (b) in **Figure 4** is too nosy above the target despite the apparent accommodation of the zero dips along the interval. Finally, result (c) is promising, presenting a good lateral resolution and a near perfect accommodation of the zero dips along the interval that was imaged. It must be remembered the result (c) is not the result of a remigration *imaging*, just a (poor) *mapping*, something that an interpreter can let it go before any further enhancement.

Let us elaborate this last observation a little further. **Figure 5** depicts two FK spectra of the results (a) and (c) of **Figure 4**, respectively, for comparison. It is clear why in **Figure 5a,** which is the result for the conventional Kirchhoff migration of the VSP data of **Figure 4**, the zero (and near zero) dips are completely accommodated along the section imaged: these events concentrate around the origin of the spectrum, as expected. As for the FK spectrum in **Figure 5b,** the spectrum section is virtually similar to the first one, but with some indication that residual dip, not at all accommodated, presents some dislocation to the right.

Figure 6 depicts the main difference between the surface seismic and VSP acquisition when one deal with the remigration problem in time. Since remigration in time is just a refocusing operator (Oliveira et al., 2023), we are

free to perform the main calculations superposing input

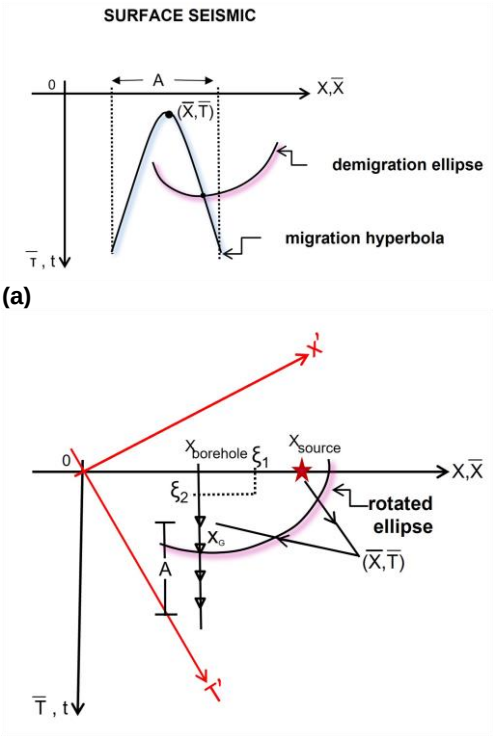

Figure 6 – The reference systems used for remigration. (a) Surface seismic. (b) VSP.

and output domains, respectively, as if they were homologues. For surface seismic (**Figure 6a**), the diffraction hyperbola is then calculated for the input domain (blue hyperbola). For every traveltime sample, which is function of ξ, and is mapped inside aperture A, one demigration is then performed (red ellipse). The result is positioned at $(\tilde{x},\tilde{\tau})$ in the output domain. As showed in Oliveira et al. (2023), this represents an *imaging* condition.

For the remigration case (**Figure 6b**), the situation is completely different, since in this case the locus of the imaging ellipses is rotated. Outcome new research shall use the *imaging* procedure with the following inplanat for the VSP problem:

$$t = t_{RM}(x;\tilde{x},\tilde{\tau}) = \frac{2\xi_2}{v_{RMS}} - \frac{2}{v_{RMS}}\frac{h_1 h_2}{\gamma_2}(x-\xi_1) + \frac{2}{\gamma_2 v_{RMS}}\sqrt{\left(\frac{v_{RMS}\tilde{\tau}_D}{2}\right)^2\left[(h_1^2+h_2^2)-\left(\frac{v_{RMS}\tilde{\tau}_D}{2}\right)\right](x-\xi_1)^2+\gamma_0\gamma_2}. \quad (8)$$

Eq. (8) is the formal solution of Eq. (6), which was recast as a second-degree equation with respect to $\left(\frac{v_{RMS}\tau}{2}-\xi_2\right)$ as the main variable for this present solution and the "+" option for its root represents the trajectories of rotated ellipses as expected in the input domain. It must be noticed that Eq. (8) is a general solution, to which the remigration inplanat for the surface seismic is a particular case in the input domain.

Conclusions

We have presented an application of a Kirchhoff-type time remigration imaging to target-oriented data. We tested this technology using surface data and in one data set derived from a synthetic VSP acquisition.

In this work the VSP example was obtained as a *mapping* solution. Future applications of Eq. (3) for VSP shall use Eq. (8) in Eq. (3) as inplanat for the *imaging* procedure.

Acknowledgments

The first author would like to thank Agência Nacional de Mineração – ANM/MT/Brazil for the permission to take part in this work. The second author would like to thank Oriti Solutions – São Paulo/Brazil for the permission to take part in this work.

References

Grech, M. G. K.; Lawton, D. C.; Cheadle, S., 2001. Integrated pre-stack depth migration of VSP and surface seismic data. *Recorder*, 26, nº 09.

Harwijanto, J. A.; Wapenaar, C. P. A.; Berkhout, A. J., 1987. VSP migration by single shot record inversion. First Break, **5**, nº 07, 247-255.

Hubral, P.; Tygel, M.; Schleicher, J., 1996a. Seismic image waves. *Gephysics J. Int.*, **125**, 431-442.

Hubral, P., Schleicher, J. & Tygel, M., 1996b. A unified approach to 3-D seismic reflection imaging-Part I: Basic concepts, *Geophysics*, **61**, 742-758.

Li, W.; Mao, W.; Liang, Q., 2023. Imaging of vertical seismic profiling using weighted generalized Radon transform migration in dip-angle domain. *Front. Earth Sci*. 10:974371. doi: 10.3389/feart.2022.974371.

Oliveira, A. S.; Lourenço, J.; Ferreira, C. A. S., 2023.Kirchhoff time-remigration and time-to-depth conversion – preliminary results and possible applications. 18th Int. Congress of the Brazilian Geophys. Soc.

OpenAI. (2025). Gemini. https://www.google.com. VSP+migration.

Schleicher, J.; Bagaini, C., 2003. Controlling Amplitudes in 2.5D common-shot migration to zero offset. Wave Inversion Technology.

Stewart, R. R., 2001. VSP: An in-depth seismic understanding. *Recorder*, 27, nº 07.

Tygel, M., Schleicher, 3. & Hubral, P., 1996. A unified approach to 3-D seismic reflection imaging-Part IT: Theory, *Geophysics*, **61**, 759-775.

Tygel, M.; Schleicher, J.; Hubral, P.; Santos, L. T., 1998.2.5D true-amplitude Kirchhoff migration to zero-offset in laterally inhomogeneous media. *Geophysics*, 63, 557-573.